Rare Earth Element (REE) Lanthanum doped zinc oxide (La: ZnO) nanomaterials: Synthesis Structural Optical and Antibacterial Studies

A. Manikandan[1*], E. Manikandan[1,6-7≠], B. Meenatchi[2], S. Vadivel[3], S. K. Jaganathan[4-5], R. Ladchumananandasivam[8], M. Henini[6-7,9], M. Maaza[6-7], Jagathrakshakan Sundeep Aanand[1]

[1]Dept. of Chemistry & Central Research Laboratory, Bharath Institute of Higher education and Research (BIHER), Bharath University, Chennai–600073, Tamil Nadu (TN), **India**
[2]PG & Research Dept. of Chemistry, Bishop Heber College, Tiruchirappalli-620017, TN, **India**
[3] Dept. of Chemistry, PSG College of Technology, Coimbatore - 641004, **India**
[4] Faculty of Applied Sciences, Ton Duc Thang University, Ho Chi Minh City 70000, **Vietnam**
[5]IJNUTM Cardiovascular Engineering Centre, Dept. of Clinical Sciences, Faculty of Biosciences and Medical Engineering, Universiti Teknologi Malaysia, Johor Bahru, **Malaysia**
[6]UNESCO UNISA Africa Chair in Nanosciences & Nanotechnology, College of Graduate Studies, University of South Africa, Muckleneuk Ridge, PO Box 392, Pretoria, **South Africa**
[7]Nanosciences African Network (NANO-AFNET), iThemba LABS-National Research Foundation, 1 Old Faure Road, Somerset West, PO Box: 722, Cape Town, 7129, **South Africa**
[8]Dept. of Textile & Chemical Engineering & P. G. Programme in Mechanical Engineering, Centre of Technology, Federal University of Rio Grande do Norte, Natal, **Brazil**
[9]School of Physics and Astronomy, Nottingham Nanotechnology and Nanoscience Center, University of Nottingham, Nottingham, NG7 2RD, **United Kingdom**

Abstract

Lanthanum (La) doped zinc oxide (ZnO) nanomaterials ($La_xZn_{1-x}O$, x = 0.0, 0.03, 0.05, 0.07 M) were synthesized via co-precipitation method using zinc acetate, lanthanum nitrate as precursors, octylamine as capping and reducing agent. The structures, morphologies, optical activity and antibacterial properties of $La_xZn_{1-x}O$ were investigated by powder X-ray diffraction (XRD), Fourier transform infrared (FT-IR) spectroscopy, High resolution scanning electron microscopy (HR-SEM), Energy dispersive X-ray (EDX), UV-Visible, Photoluminescence (PL) spectroscopy. The antibacterial activities of $La_xZn_{1-x}O$ were tested by modified disc diffusion method. The XRD results showed that the La^{3+} ions were successfully incorporated into the ZnO host, and the

[1*,≠] Corresponding author: mkavath15@gmail.com ; maniphysics@gmail.com (Prof. Manikandan)

products were well-crystalline. The average size of undoped and doped La-doped ZnO was found to be in the ranges from 15.64 to 10.18 nm. In addition, the sphere-like nanoparticles morphology of $La_xZn_{1-x}O$ was confirmed by HR-SEM images. The band gap of La-doped ZnO nanoparticles were varied with the La^{3+} ions doping concentration. In addition, increasing the doping concentration of La^{3+} ions in ZnO increases the defects in ZnO lattice and hence resulting red-shift in UV emission, which indicate the presence of narrow band-gap in doped nanoparticles.

Keywords: Chemical route; La-doped ZnO; Nanomaterials; Optical; Structural; Antibacterial activity.

1. Introduction

The nanostructured metal oxides show unique properties like semiconducting, insulating behavior etc., over their same bulk materials [1-3]. In recent years, zinc oxide (ZnO) nanomaterials have attracted much consciousness within the scientific researchers owing to its low-cost, easy fabrication, photocatalytic activity, wide band-gap semiconductor [4-9], unique optical, magnetic and electronic properties etc. [10-12] ZnO materials are a translucent piezo electric and electro conductive materials. In addition, ZnO materials act as an admirable ultraviolet absorber and antibacterial agent. ZnO materials possess band gap energy of 3.37eV and great excitation binding energy of 60 meV at room temperature (RT), which provides more efficient excitonic emission even at high temperature. ZnO materials have been synthesized through numerous methods, which include chemical precipitation, sol-gel, microwave radiation and hydrothermal methods, etc.

The doping of ZnO materials with different types of metallic ions [12-15] enhances its optical, magnetic and conducting properties. Such modified ZnO materials may be used as a base material for magnetic semiconductors, solar cells, field-effect transistors, gas sensors, light-emitting materials, photo-catalysts and biological systems (bio-imaging, drug delivery, etc.) [16-17]. Furthermore, doping with rare earth elements (e.g., La, Tb, Er, Eu, Dy and Sm) provides many interesting properties of ZnO materials, which includes the efficient modulation of the emission in the visible range owing to their unique optical properties. Above all, Lanthanum (La)-doped ZnO materials shows excellent gas sensitivity and photocatalytic activity.

Present research is focused on investigating the result of La doping concentration on the structure and optical properties of undoped and La doped ZnO materials prepared by a facile chemical precipitation method using zinc acetate as source of Zn^{2+} ions and lanthanum nitrate as source of La^{3+} ions. The chemical precipitation route to synthesis of La doped ZnO materials has several advantages like high quality, low-processing cost, quite low temperature and higher yield etc. in comparison with other methods.

2. Materials and Methods

2.1. Synthesis of $La_xZn_{1-x}O$ (x= 0.0, 0.03, 0.05, 0.07 M) nanomaterials

Undoped and La-doped zinc oxide ($La_xZn_{1-x}O$) nanomaterials were prepared by co-precipitation method using zinc acetate and lanthanum nitrate as metal precursors (Zn, La respectively) and octylamine as reducing and capping agent. To the solution of 0.1M of zinc acetate in 100 mL methanol, 1 mL of octylamine was added then stirred continuously for 24 h at room temperature to obtain homogenous precursor solution. Later, different moles (0.03, 0.05, 0.07 M) of lanthanum nitrate ($LaNO_3$) were added into the above precursor solutions and stirred

for 3 h. Finally, 3 M NaOH was added drop wise into the obtained solution until pH attains 12. The resulting solution was aged about 1h and the precipitates were collected and washed using distilled water to remove the unreacted reagents. The slurry was dried in an oven at 80 ˚C for about 10 h and annealed at 400 ˚C for 2 h. The pure ZnO sample was prepared by adopting the same procedure without the addition of $LaNO_3$.

2.2. Characterization

X-ray diffraction (XRD) pattern was recorded at room temperature using PAN analytical X′Pert PRO equipment using CuK_α irradiation as found the wavelength (λ = 1.5418 Å). The morphology and elemental composition analysis of the samples were investigated by High resolution scanning electron microscope using (JEOL, JSM-67001). The optical absorption spectra were recorded by UV-Vis absorption spectrometer (Perkin Elmer T90 Spectrophotometer). Room-temperature photoluminescence spectral measurements were carried out using JY Fluorolog 3-11 spectrometer. The solid phase FT-IR spectrum in KBr pellet technique was recorded with (FT-IR; JASCO, Model 6300).

2.3. Antibacterial activity

Antimicrobial activity of the prepared samples was tested in both gram-negative and gram-positive bacteria namely *Staphylococcus aureus*, *Proteus mirabilis*, S*almonella typhii* and *Bacillus subtilis* by disc diffusion method with small modifications. The 24 h bacterial cultures were swabbed in a Muller Hinton agar amended plates. Whatmann filter paper discs of 3 mm diameter were impregnated with 100 μL of the solution containing samples ($La_xZn_{1-x}O$; x = 0.0, 0.03, 0.05, 0.07 M) and these discs could evaporation for 1 h. Reference standard discs were prepared with ampicillin (10 μg/mL) to compare the antibacterial activity of the samples. After

drying, the discs were placed in swabbed bacterial plates and incubated at 28 °C for 24 h. After incubation, plates were examined for clear zone around the discs. A clear zone more than 2 mm in diameter was taken for antibacterial activity.

3. Results and Discussion

3.1. Powder X-ray diffraction (XRD) analysis

Figure 1 showed the powder XRD patterns of $La_xZn_{1-x}O$ (x = 0.0, 0.03, 0.05, 0.07 M) nanoparticles with 2θ range from 30^o to 75^o at room temperature. The diffraction peaks and their relative intensities of both undoped and La doped ZnO samples were in good agreement with the standard JCPDS card no. 36-1451. Hence, the observed patterns can be clearly endorsed to the presence of hexagonal wurtzite structure. Furthermore, in Figure 1, no additional XRD peaks were found which clearly indicates the absence of La oxide or Zn-La alloys formation. Hence, it was clear that the introduction of dopant could not alter the crystal structure, whereas it dispersed uniformly in the ZnO matrix [18].

In addition, from Figure 1, it was found that the most intense peak of doped ZnO materials shifted towards higher θ value. This shift is due to the internal strain developed by the substitution of Zn^{2+} (host ions) by La^{3+} dopant ions [19-22]. The higher intensity of all peaks suggested that the material was in highly crystalline nature.

The lattice parameter was calculated using the formula given in Eq. (1):

$$\sin^2\theta = \frac{\lambda^2}{4}\left[\frac{4}{3}\left(\frac{h^2+hk+k^2}{a^2}\right)+\frac{l^2}{c^2}\right] \qquad \text{---- (1)}$$

where θ is the diffraction angle, λ, the incident wavelength (λ = 0.1540 nm), h, k, and l are Miller's indices. The obtained lattice parameter values of both undoped and La-doped ZnO were

listed in Table 1. From Table 1, it was clear that the lattice parameter values of La-doped ZnO materials, are less in comparison with those for pure ZnO materials, due to the shift of XRD peaks towards higher 2θ values for doped ZnO nanoparticles. Similar lattice parameter values (a = 3.251001 ± 0.000064 Å c = 5.208817 ± 0.000161 Å for undoped ZnO materials and a = 3.249680 ± 0.000054 Å, c = 5.205810 ± 0.000140 Å) has been reported by Goel *et al*. [23]. Moreover, it was clear that La-doping changed the lattice parameters values, but the crystal system (hexagonal) and space group (P63mc) remain unchanged.

The average crystallite size was calculated using Scherer formula given in Eq. (2):

$$L = \frac{0.89\lambda}{\beta \cos\theta} \qquad \text{----(2)}$$

where L is the crystallite size, λ, the X-ray wavelength, θ, the Bragg diffraction angle and β, the full width at half maximum (FWHM). The average crystallite sizes of undoped and doped ZnO were listed in Table 1. The average crystallite sizes of undoped and La-doped ZnO materials were calculated to be 15.64 nm (x = 0M), 13.28 nm (x = 0.03M), 11.46 nm (x = 0.05M), 10.18 nm (x = 0.07 M) respectively. Thus, the particle size decreases because of La doping in ZnO nanostructures. This reduction in the crystallite size is due to distortion in the ZnO matrix by La^{3+} dopant ions, which decreases the rate of growth of ZnO.

3.2. Fourier transform infrared (FT-IR) spectral Analysis

The FT-IR spectra of $La_xZn_{1-x}O$ (x = 0.0, 0.03, 0.05, 0.07 M) nanoparticles were shown in Figure 2. The strong intensity band at around 505 cm^{-1} clearly indicates the Zn-O stretching vibration and the band at 607 cm^{-1} confirms the presence of ZnO and La. The 880 cm^{-1} corresponds to N-O deformation vibration. It was noted from the FT-IR data that the Zn-O

vibrational mode was more prominently observed and this clearly concludes a strong doping exist in $La_xZn_{1-x}O$.

3.3 High Resolution-Scanning electron microscopy (HR-SEM) studies

The surface morphology of $La_xZn_{1-x}O$ (x = 0.0, 0.03, 0.05, 0.07 M) materials was examined by HR-SEM analysis and showed in Figure 3. HR-SEM images clearly indicated the sphere-like morphology of nanoparticles. Furthermore, from the Figure 3 it was noted that as La concentration increases, particle size of the samples decreased, which was consistent with the XRD results.

3.4. Energy dispersive X-ray (EDX) analysis

The chemical purity and elemental composition of the $La_xZn_{1-x}O$ materials were investigated by Energy Dispersive X-ray analysis (EDX) as shown in Figure 4. The EDX results showed the presence of Zn, O and La by the appearance of their corresponding peaks without any other characteristic peaks and suggested that the prepared samples do not contain any other element impurities.

3.5. UV–Vis absorption spectroscopy

The optical properties of $La_xZn_{1-x}O$ materials with various doping concentrations were investigated by UV–Vis absorption spectra which are shown in Figure 5. From Figure 5, it was noted that the band-edge absorption of the synthesized $La_xZn_{1-x}O$ materials located at around 366-373 nm (in near UV region). The optical band gap of Eg is calculated using the following Eq. 3 [23, 24].

$$\alpha = A(h\nu - E_g)^n/h\nu \qquad \text{---------- (3)}$$

where A and n is a constant, equal to 1/2 for the direct band gap semiconductor. The calculated band gaps of the synthesized $La_xZn_{1-x}O$ materials were shown in Figure 6. It was noted that the lanthanum doping concentration had significant effects on the band gaps of synthesized $La_xZn_{1-x}O$ materials. When the doping concentration of lanthanum changes from 0 to 0.07 M, the value of E_g is decreased from 3.07 to 2.91 eV. When a Zn site in ZnO was occupied by a La atom, there were two main effects were observed: (1) The impurity bands closer to the lower edge of the conduction band, which was created by substituted La and (2) The obtained band-gap exhibit narrow, due to the strong orbital coupling between La and O. The results illustrated that La doping concentration plays vital role in tuning the band gap of the synthesized $La_xZn_{1-x}O$ materials. Furthermore, the existence of extended tail band (from 450 to 800 nm) in the UV spectra of La-doped ZnO nanoparticles (Figure 5) showed its optical capability almost in the whole range of visible light spectra. The sp–d exchange interactions between the conduction band electrons and the localized d electrons of the La^{3+} ions, which substitute Zn^{2+} ions lead to the broad absorption in visible light range [25]. In addition, the s–d and p–d exchange interactions cause a negative and a positive correction to the conduction band and the valence band edges individually, resulting in strong visible light absorption of the La-doped ZnO materials [26, 27]. Hence, La- doping in ZnO host can introduce the impurity energy levels in band gap and expands its visible light response, which is favorable for several potential applications. These results indicate that the La doped ZnO nanoparticles can absorb in UV as well as in the visible region of the solar light suggesting that the La doped ZnO nanoparticles could be applied as a visible light photocatalyst [28].

3.6. Photoluminescence spectral analysis

The PL spectra of $La_xZn_{1-x}O$ materials (x = 0, 0.03, 0.05 and 0.07) was showed in Figure 7. The emission bands around at 410 nm (UV emission) were observed due to the recombination of the free excitons in ZnO [29-31]. Small variations (409.95, 410.15, 410.14, 410.25 nm) in the positions of UV emission bands in PL spectra of $La_xZn_{1-x}O$ materials could be attributed to the impact of lanthanum doping concentration. The position of UV emission bands slightly increases as lanthanum doping concentration increases, but the intensity of the peaks decreased. Hence, the UV emission had a red shift, since the doping concentration of lanthanum increases. In addition, the shift in the emission spectra for undoped and doped ZnO may be attributed, due to the strain created in the crystal lattice to accommodate larger La atoms in ZnO. Furthermore, the deep-level emission in region from 490 nm to 540 nm was due to the intrinsic deep-level defects and extrinsic impurities in ZnO [32-40].

3.7. Antibacterial Activities

The antibacterial activities of synthesized $La_xZn_{1-x}O$ materials were tested against the human pathogens like *P.mirabilis*, *S.typhi, S.aureus, B.subtilis* with reference to Ampicillin. The antibacterial activity values are listed in Table 2. From the results, it was observed that the synthesized $La_xZn_{1-x}O$ materials showed desired activity against *P. mirabilis* and *S. typhi.* Furthermore, when La concentration increases, activity of $La_xZn_{1-x}O$ materials against *P. mirabilis* and *S. typhi* increases to higher extent, while $La_xZn_{1-x}O$ materials showed no activity against *S. aureus, B. subtilis,* P. *mirabilis* and *S. typhi* causes kidney stone and typhoid fever respectively. Hence, the synthesized $La_xZn_{1-x}O$ can be used in the treatment of kidney stone and Typhoid Fever.

4. Conclusions

In summary, La-doped ZnO ($La_xZn_{1-x}O$: x = 0.0, 0.03, 0.05, 0.07 M) nanoparticles have been synthesized by chemical precipitation route. From XRD measurements, it was confirmed that the particle size of the synthesized $La_xZn_{1-x}O$ materials decreases with increasing La concentrations and possess hexagonal wurtzite structure. In addition, the sphere-like morphology was revealed by HR-SEM and HR-TEM analysis. The elemental composition was confirmed by EDX analysis. Furthermore, it was found that La^{3+} ions were successfully incorporated into the ZnO lattice, and the red shift was appeared in PL spectra for doped nanoparticles compared with undoped one. The band gap energies of doped nanoparticles were decreased from 3.07 eV to 2.91 eV with increasing the lanthanum doping concentration. Hence, these results indicated that the lanthanum doping concentration plays an important role in tuning the size, band gap and photoluminescence property of the ZnO nanoparticles. In addition the synthesized $La_xZn_{1-x}O$ materials possess significant antibacterial activity against *P.mirabilis, S.typhi* and used for treatment of kidney stone and typhoid fever.

ACKNOWLEDGMENT

The author's A. M & E. M would like to thank for the institute founder Dr. S. Jagathrakshakan & esteemed advisor Shri. V. Murthy, IAS, Bharath University, BIHER (Bharath Institute of Higher Education & Research) for their inestimable support & constant encouragement, laboratories chemicals, scientific computers facilities and future financial support for the upcoming work. In addition, Dr. S. Bhuminathan, Registrar are acknowledged.

References

[1]. B. Meenatchi, V. Sathiya Lakshmi, A. Manikandan, V. Renuga, A. Sharmila, K. R. Nandhine Deve & Saravana Kumar Jaganathan, Protic ionic liquid assisted synthesis and characterization of ferromagnetic cobalt oxide nanocatalyst, J. Inorg. Organomet. Polym. 27 (2017) 446–454.

[2] A. Manikandan, M. Durka, K. Seevakan, S. Arul Antony, A novel one-pot combustion synthesis and opto-magnetic properties of magnetically separable spinel $Mn_xMg_{1-x}Fe_2O_4$ ($0.0 \leq x \leq 0.5$) Nanophotocatalysts, J. Supercond. Nov. Magn. 28 (2015) 1405-1416.

[3]. A. Manikandan, M. Durka, S. Arul Antony, A novel synthesis, structural, morphological, and opto-magnetic characterizations of magnetically separable spinel $Co_xMn_{1-x}Fe_2O_4$ ($0 \leq x \leq 1$) nano-catalysts, J. Supercond. Nov. Magn. 27 (2014) 2841-2857.

[4] E. Manikandan, M. K. Moodley, S. S. Ray, B. K. Panigrahi, R. Krishnan, K. G. M. Nair, A. K. Tyagi, Zinc oxide epitaxial thin-film deposited over carbon on various substrates by PLD technique, J. Nanosci. Nanotech. 10 (2010) 5601-5611.

[5] J. F. Zhu and Y. J. Zhu, Microwave-assisted one-step synthesis of polyacrylamide-metal (M = Ag, Pt, Cu) nanocomposites in ethylene glycol, J. Phys. Chem. B 110 (2006) 8593-8597.

[6] N. C. S. Selvam, A. Manikandan, L. John Kennedy, and J. Judith Vijaya, Comparative investigation of zirconium oxide (ZrO_2) nano and microstructures for structural, optical and photocatalytic properties, J. Colloid Interf. Sci. 389 (2013) 91-98.

[7] A. H. Shah, E. Manikandan, M B. Ahmed. Enhanced bioactivity of Ag/ZnO nanorods-a comparative antibacterial study. 2013. J. Nanomed. Nanotech. 4 (2013) 6p.

[8] J Kennedy, PP Murmu, J Leveneur, A Markwitz, J Futter. Controlling preferred orientation and electrical conductivity of zinc oxide thin films by post growth annealing treatment, Applied Surface Science 367 (2016) 52-58.

[9] E. Manikandan, J. Kennedy, G. Kavitha, K. Kaviyarasu, M. Maaza, B.K. Panigrahi, U. Kamachi Mudali. "Hybrid Nanostructured Thin-Films by PLD for Enhanced Field Emission Performance for Radiation Micro-Nano Dosimetry Applications. 2015. J. Alloys & Comps 647 (2015) 141-145.

[10]. J Kennedy, B Sundrakannan, RS Katiyar, A Markwitz, Z Li, W Gao, Raman scattering investigation of hydrogen and nitrogen ion implanted ZnO thin films, Current Applied Physics 8 (2008) 291-294

[11]. PP Murmu, J Kennedy, GVM Williams, BJ Ruck, S Granville, SV Chong, Observation of magnetism, low resistivity, and magnetoresistance in the near-surface region of Gd implanted ZnO, Applied Physics Letters 101 (2012) 082408

[12]. J Kennedy, GVM Williams, PP Murmu, BJ Ruck, Intrinsic magnetic order and inhomogeneous transport in Gd-implanted zinc oxide, Physical Review B 88 (2013) 214423

[13] B. Sathyaseelan, E. Manikandan, K. Sivakumar, J. Kennedy, M. Maaza. Enhanced visible photoluminescent and structural properties of ZnO/KIT-6 nanoporous materials for white light emitting diode (w-LED) application, J. Alloys Compds 651 (2015) 479-482.

[14] E. Hema, A. Manikandan, P. Karthika, S. Arul Antony, B. R. Venkatraman, A novel synthesis of Zn^{2+}-doped $CoFe_2O_4$ spinel nanoparticles: Structural, morphological, opto-magnetic and catalytic properties, J. Supercond. Nov. Magn. 28 (2015) 2539–2552.

[15] B. Meenatchi, K. R. Nandhine Deve, A. Manikandan, V. Renuga, and V. Sathiyalakshmi, Protic ionic liquid assisted synthesis, structural, optical and magnetic properties of Mn-doped ZnO nanoparticles, Adv. Sci. Eng. Med. 8 (2016) 653-659.

[16]. J Kennedy, PP Murmu, E Manikandan, SY Lee, Investigation of structural and photoluminescence properties of gas and metal ions doped zinc oxide single crystals, Journal of Alloys and Compounds 616 (2014) 614-617

[17]. F Fang, J Kennedy, DA Carder, J Futter, P Murmu, A Markwitz, Modulation of field emission properties of ZnO nanorods during arc discharge, Journal of nanoscience and nanotechnology 10 (2010) 8239-8243

[18] J. T. Chen, J. Wang, F. Zhang, G. A. Zhang, Z.G. Wu, P.X. Yan, The effect of La doping concentration on the properties of zinc oxide films prepared by the sol–gel method, J. Crys. Growth 310 (2008) 2627–2632.

[19] S. Goel, N.Sinha, H. Yadav, A.J. Joseph, B.Kumar, Experimental investigation on the structural, dielectric, ferroelectric and piezoelectric properties of La doped ZnO nanoparticles and their application in dye-sensitized solar cells, Physica E 91 (2017) 72–81.

[20] M. Poloju, N Jayababu, E. Manikandan, MVR Reddy. Enhancing the Isopropanol gas sensing performance of SnO_2/ZnO core/shell nanocomposite gas sensor. Journal of Materials Chemistry C. 5 (2017) 2662-2668. DOI: 10.1039/C6TC05095F.

[21] A.S.H. Hameed, C. Karthikeyan, A.P. Ahamed, N. Thajuddin, N.S. Alharbi, S.A. Alharbi, G. Ravi, *In vitro* antibacterial activity of ZnO and Nd doped ZnO nanoparticles against ESBL producing *Escherichia coli* and *Klebsiella pneumoniae*, Sci. Rep. 6 (2016) 24312.

[22] E. Manikandan, V. Murugan, G. Kavitha, P. Babu, M. Maaza. Nanoflower rod wire-like structures of dual metal (Al and Cr) doped ZnO thin films: Structural, optical and electronic properties. Materials Letters, 131 (2014) pp.225-228.

[23] J. Cao, J. Yang, Y. Zhang, L. Yang, D. Wang, M. Wei, Y. Wang, Y. Liu, M. Gao, X. Liu, Growth mechanism and blue shift of Mn^{2+} luminescence for wurtzite ZnS: Mn^{2+} nanowires, J. Phys. D Appl. Phys. 43 (2010) 075403.

[24] M. Saif, H. Hafez, A.I. Nabeel, Photo-induced self-cleaning and sterilizing activity of Sm^{3+} doped ZnO nanomaterials, Chemosphere, 90 (2013) 840-847.

[25] E. Manikandan, L Krishnakumar, K Gnanasekaran, G Mani. et.al. Effective Ammonia Detection Using n-ZnO/p-NiO Heterostructured Nanofibers. IEEE Sensors Journal 16 (2016), 2477 – 2483.

[26] A. H. Shah, E. Manikandan, MB Ahamed, D Ahmad Mir, S. Ahmad Mir, Antibacterial and Blue shift investigations in sol-gel synthesized $Cr_xZn_{1-x}O$ Nanostructures. J Lumin.145 (2014) 944-948.

[27] C. Xu, L. Cao, G. Su, W. Liu, X. Qu, Y. Yu, Preparation, characterization and photocatalytic activity of Co-doped ZnO powders, J. Alloys Compd. 497 (2010) 373-376.

[28] M. Shakir, M. Faraz, Asif Sherwani, Saud I. Al- Resayes, Photocatalytic degradation of the paracetamol drug using lanthanum doped ZnO nanoparticles and their in-vitro cytotoxicity assay, J. Lumin. 176 (2016) 159–167.

[29] D. Weissenberger, M. Durrschnabel, D. Gerthsen, F. Perez-Willard, A. Reiser, G. M. Prinz, M. Feneberg, K. Thonke, R. Sauer, Conductivity of single ZnO nanorods after Ga implantation in a focused-ion-beam system, Appl. Phys. Lett. 91 (2007) 132110.

[30] C Sasikala, N Durairaj, I Baskaran, B Sathyaseelan, M Henini, E. Manikandan, Transition metal titanium (Ti) doped $LaFeO_3$ nanoparticles for enhanced optical structural and magnetic properties. J. Alloys & Comps 712 (2017) 870-877.

[31] L. L. Yang, Q. X. Zhao, M. Willander, X. J. Liu, M. Fahlman, J. H. Yang, Effective suppression of surface recombination in ZnO nanorods arrays during the growth process, Cryst. Growth Des. 10 (2010) 1904 -1910.

[32] D. Wang, G. Xing, M. Gao, L. Yang, J. Yang, W. Tom, Defects-mediated energy transfer in red-light-emitting Eu-doped ZnO nanowire arrays, J. Phys. Chem. C 115 (2011) 22729-22735.

[33] J. Lang, J. Wang, Q. Zhang, X. Songsong, Q. Han, Y. Zhang, Hongju. Zhai, J. Cao, Y. Yan, J. Yang, Rapid synthesis and photoluminescence properties of Eu-doped ZnO nano needles *via* facile hydrothermal method, Chem. Res. Chin. Univ. 30 (2014) 538-542.

[34] L. L. Yang, Q. X. Zhao, M. Willander, X. J. Liu, M. Fahlman, J. H. Yang, Origin of the surface recombination centers in ZnO nanorods arrays by XPS, Appl. Surf. Sci. 256 (2010) 3592-3597.

[35]. E. Manikandan, G. Kavitha, J. Kennedy. Epitaxial zinc oxide, graphene oxide composite thin-films by laser technique for micro-Raman and enhanced field emission study. Ceramic International. 40 (2014) 16065-16070.

[36]. RJ Mendelsberg, J Kennedy, SM Durbin, RJ Reeves. Raman scattering investigation of hydrogen and nitrogen ion implanted ZnO thin films. Current Applied Physics. 6 (2006) 495-498.

[37]. RJ Mendelsberg, J Kennedy, SM Durbin, RJ Reeves. Carbon enhanced blue–violet luminescence in ZnO films grown by pulsed laser deposition. Current Applied Physics. 8 (2008) 283-286

[38]. F Fang, J Kennedy, J Futter, T Hopf, A Markwitz, E Manikandan, Size-controlled synthesis and gas sensing application of tungsten oxide nanostructures produced by arc discharge. Nanotechnology. 22 (2011), 335702.

[39]. J Kennedy, A Markwitz, Z Li, W Gao, C Kendrick, SM Durbin, R Reeves. Modification of electrical conductivity in RF magnetron sputtered ZnO films by low-energy hydrogen ion implantation. Current Applied Physics 6 (2006) 495-498.

[40]. AH Shah, MB Ahamed, E Manikandan, R Chandramohan, M Iydroose. Magnetic, optical and structural studies on Ag doped ZnO nanoparticles. Journal of Materials Science: Materials in Electronics 24 (2013) 2302-2308.

Figures captions

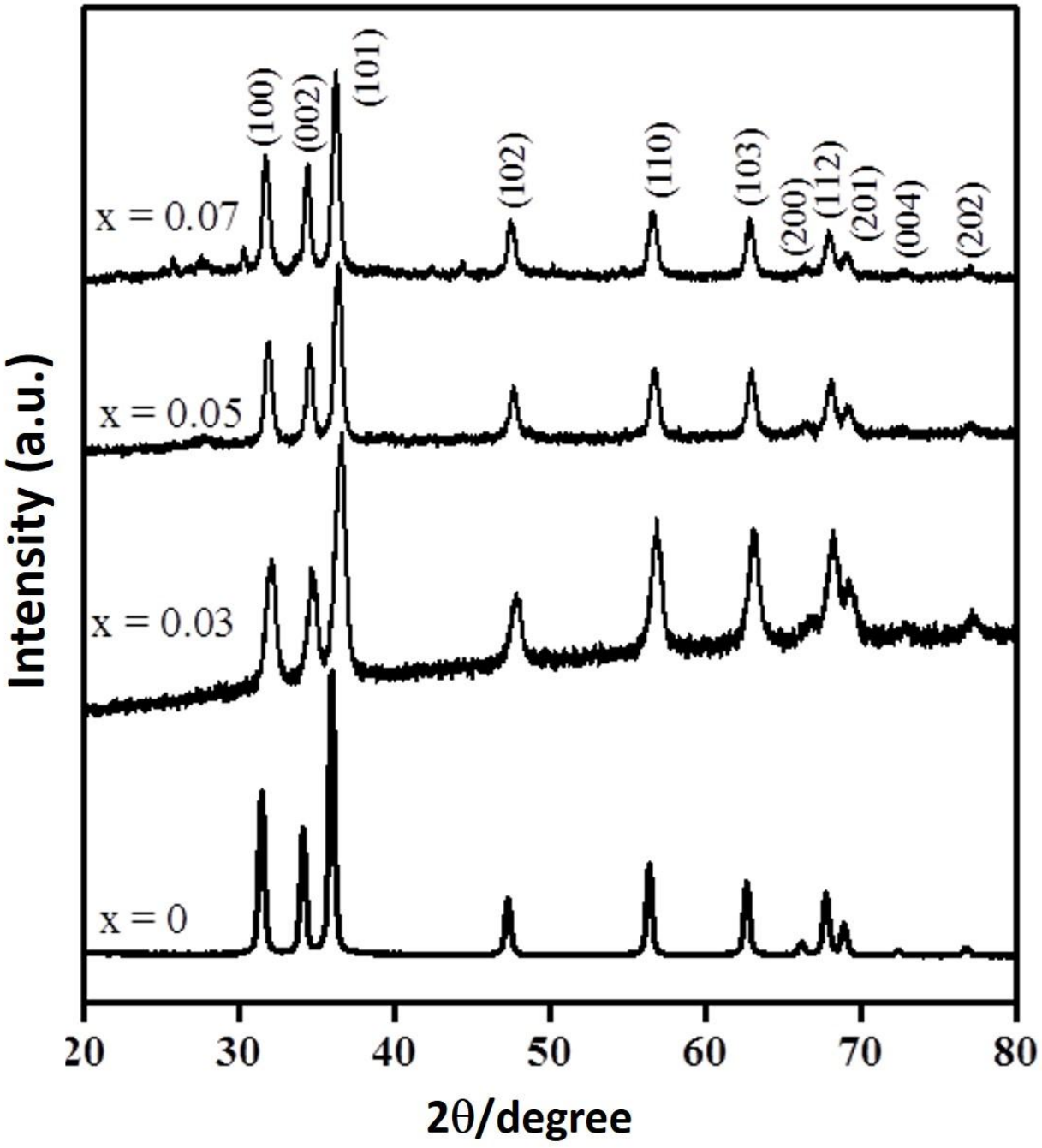

Fig. 1. Powder XRD pattern of $La_xZn_{1-x}O$ nanomaterials

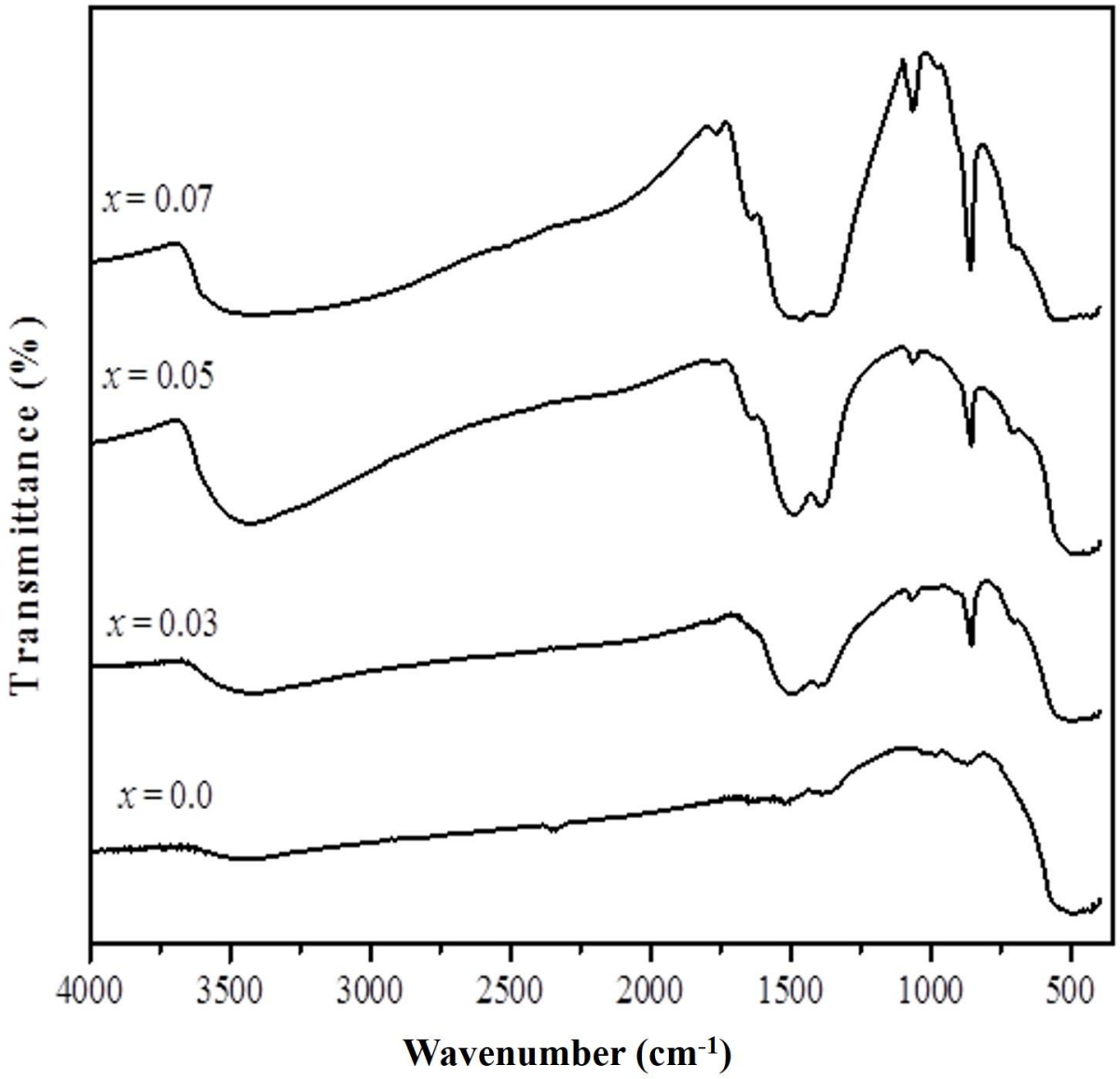

Fig. 2. FT-IR spectra of $La_xZn_{1-x}O$ nanomaterials

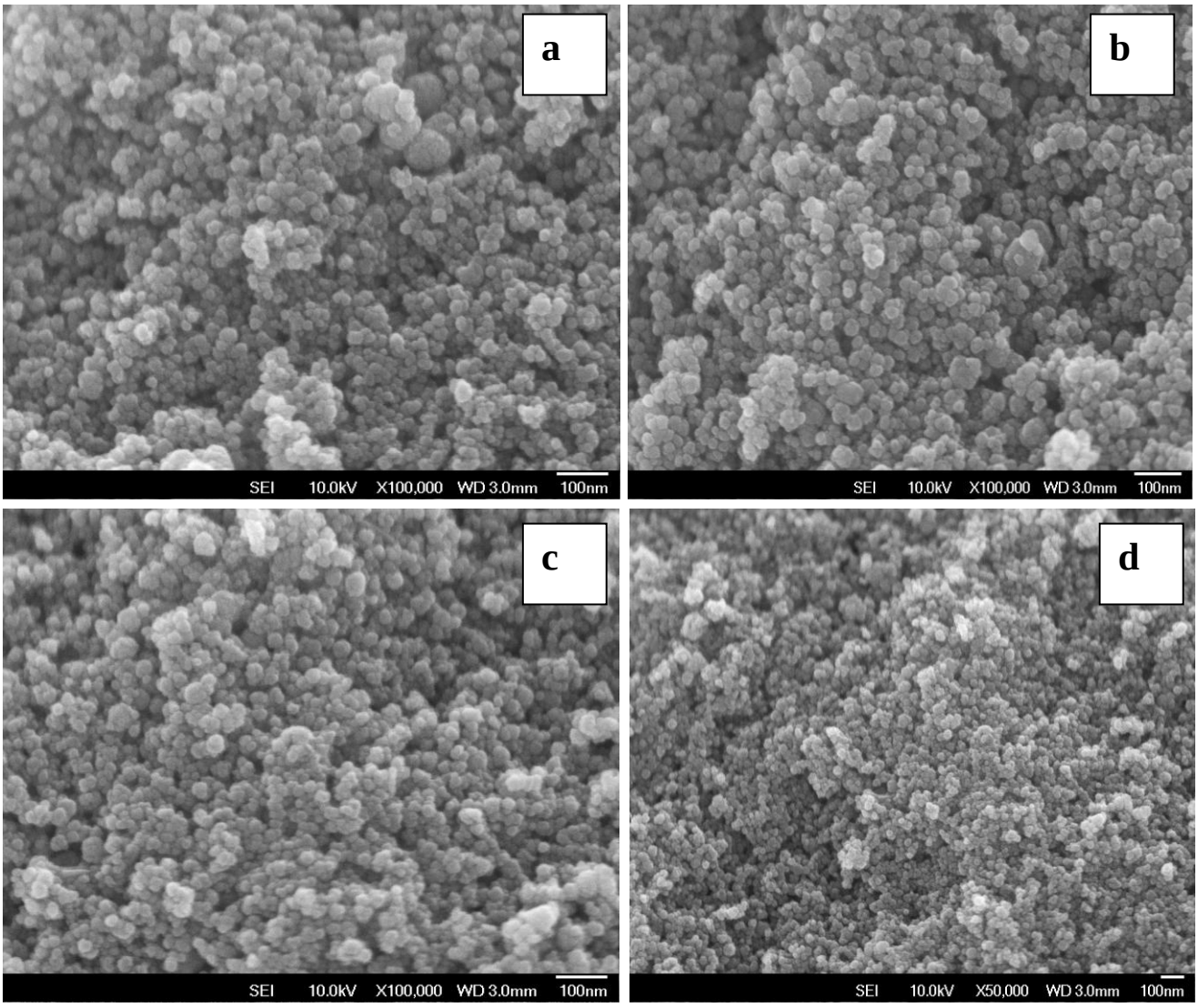

Fig. 3. HR-SEM images of $La_xZn_{1-x}O$ (a) x = 0, (b) x = 0.03, (c) x = 0.05 and (d) x = 0.07) nanomaterials

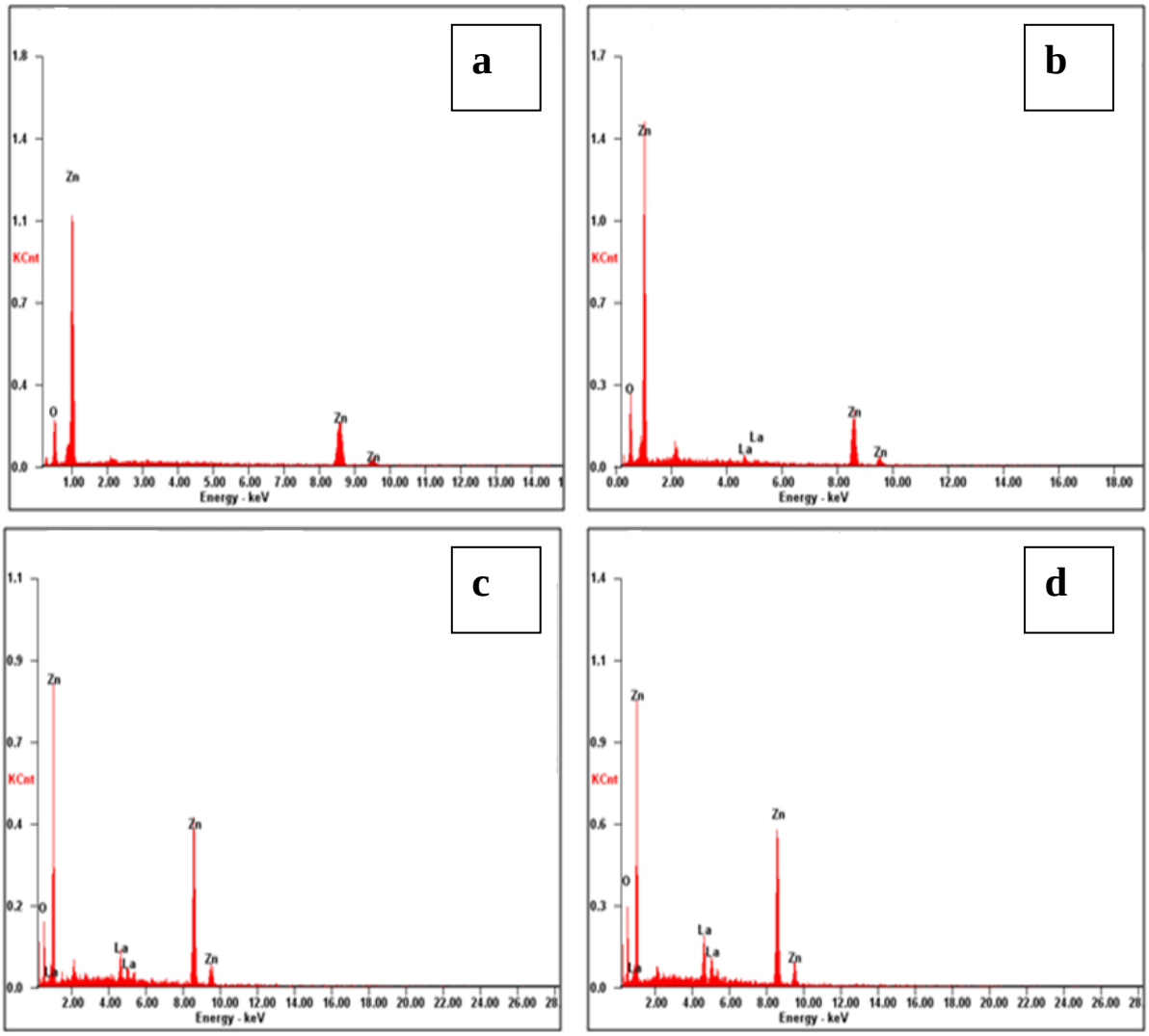

Fig. 4. EDX spectra of $La_xZn_{1-x}O$ (a) x = 0, (b) x = 0.03, (c) x = 0.05 and (d) x = 0.07) nanomaterials

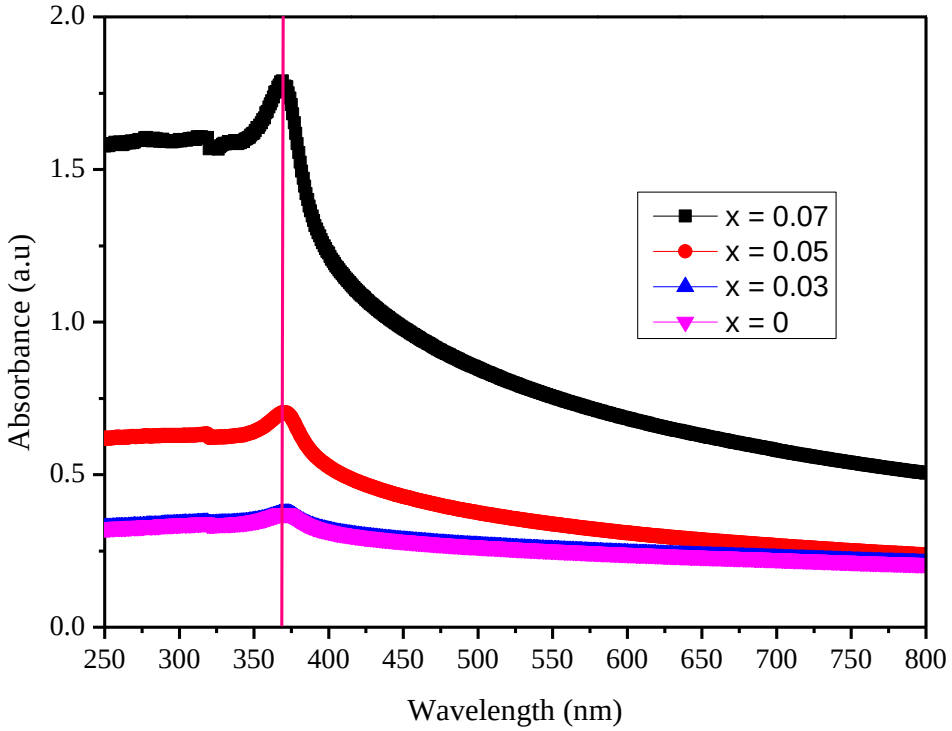

Fig. 5. Absorption spectra of $La_xZn_{1-x}O$ nanomaterials

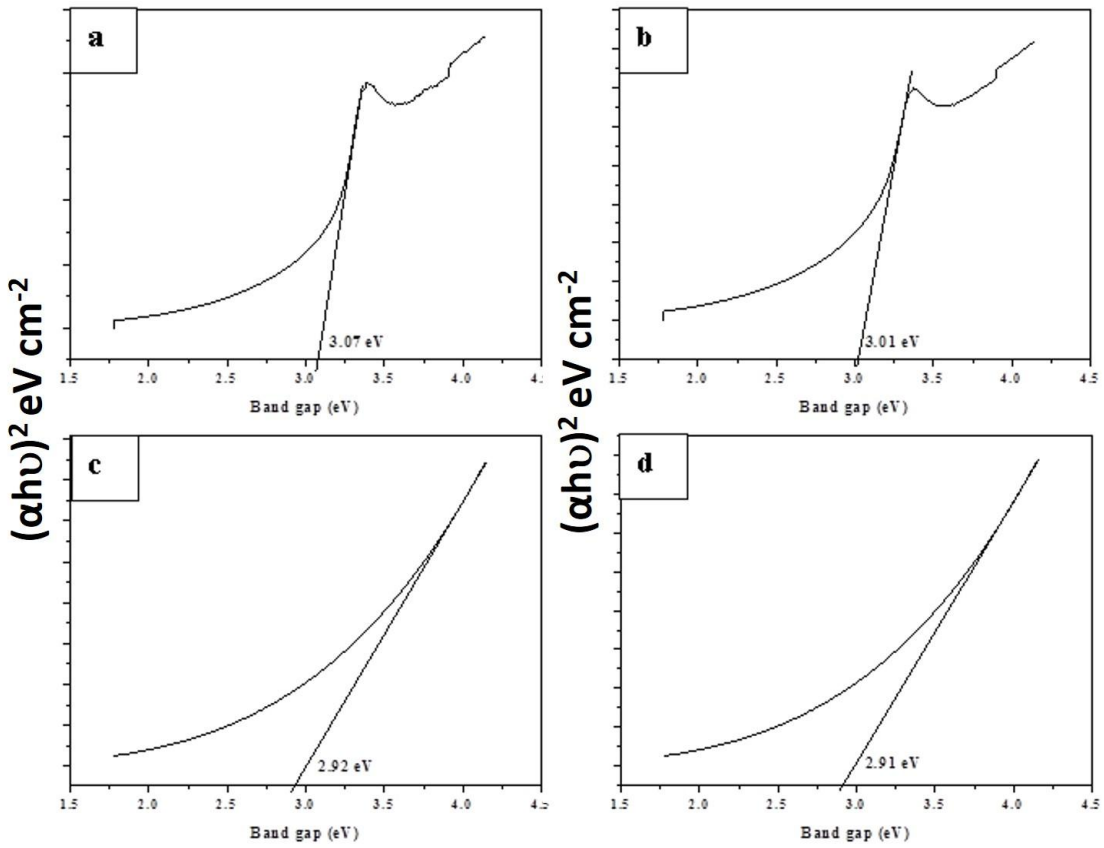

Fig. 6. Tauc plots of $(\alpha h\nu)^2$ versus hν of $La_xZn_{1-x}O$ (a) x = 0, (b) x = 0.03, (c) x = 0.05 and (d) x = 0.07) nanomaterials

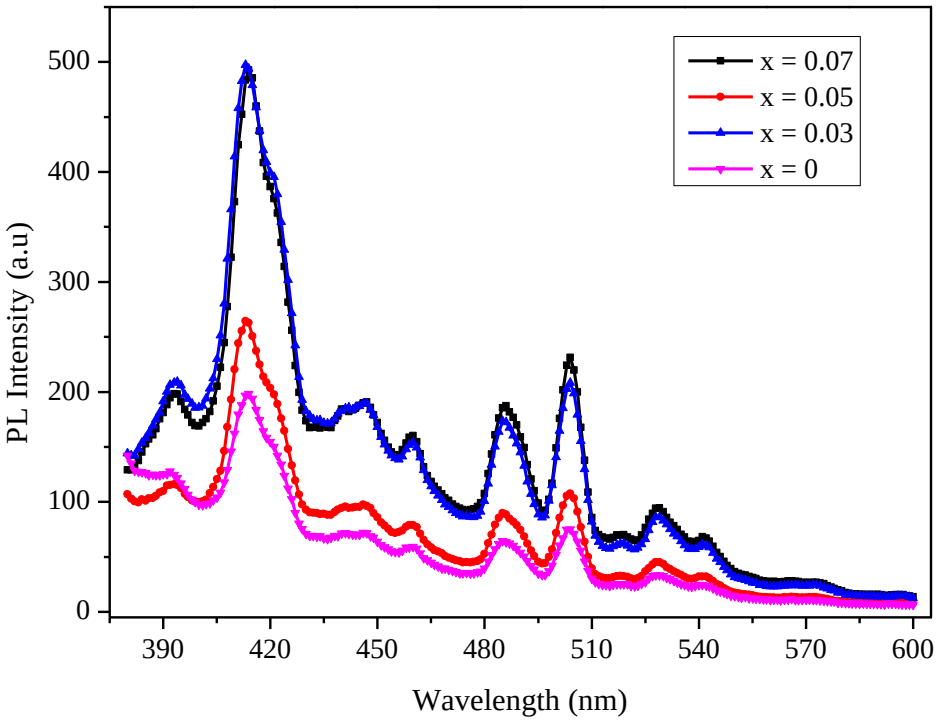

Fig. 7. PL spectra of $La_xZn_{1-x}O$ nanomaterials

Table 1. Structural parameters (Lattice constant and Crystallite size of $La_xZn_{1-x}O$ nanomaterials

La Concentration (mole %)	Lattice parameter values (Å)			Crystallite size (D) (nm)	Volume (V) $(Å)^3$
	(a)	(c)	c/a		
0	3.251	5.211	1.606	15.64	53.92
0.03	3.242	5.192	1.603	13.28	49.44
0.05	3.211	5.162	1.605	11.46	47.56
0.07	3.178	5.091	1.602	10.18	45.48

Table: 2 Antibacterial activities of $La_xZn_{1-x}O$ nanomaterials for against human pathogens

Antibacterial activities of samples were determined as zone of inhibition (in mm)				
Samples	***P. mirabilis***	***S .typhi***	***S. aureus***	***B. subtilis***
Ampicillin (C)	24	19	12	11
x = 0	7	5	0	0
x = 0.03	9	9	0	0
x = 0.05	20	15	0	0
x = 0.07	22	7	0	0

Graphical Abstract

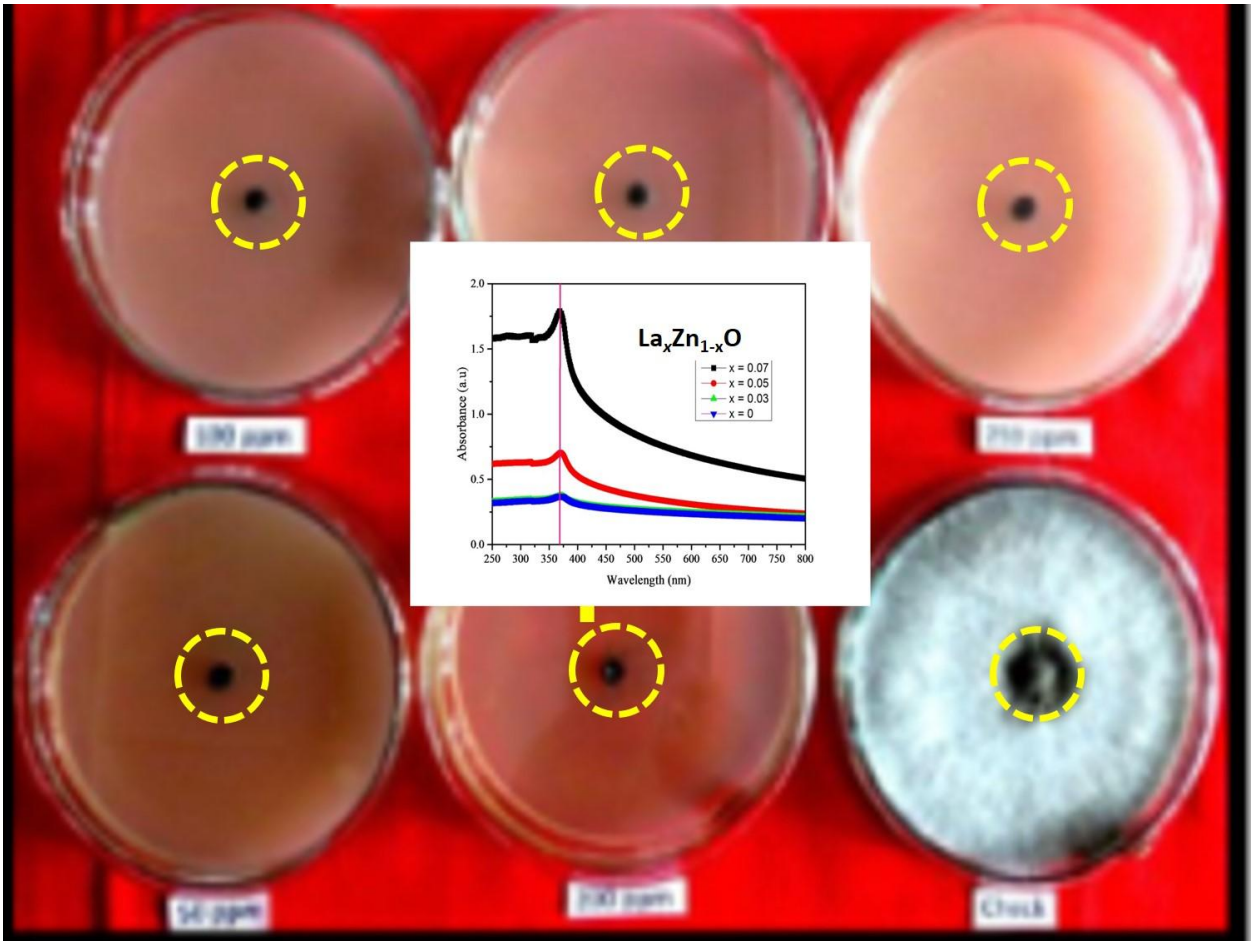

Highlights

- Enhanced optical properties La doped ZnO nanoparticles
- La-doped ZnO nanomaterials were synthesized by chemical method
- XRD, FT-IR, UV-Visible, HR-SEM, EDX, PL spectroscopy techniques were used
- The antibacterial activities of $La_xZn_{1-x}O$ were tested by modified disc diffusion method
- Average particle size of undoped and doped La-doped ZnO was found 15 to 10 nm

Graphical Abstract (for review)

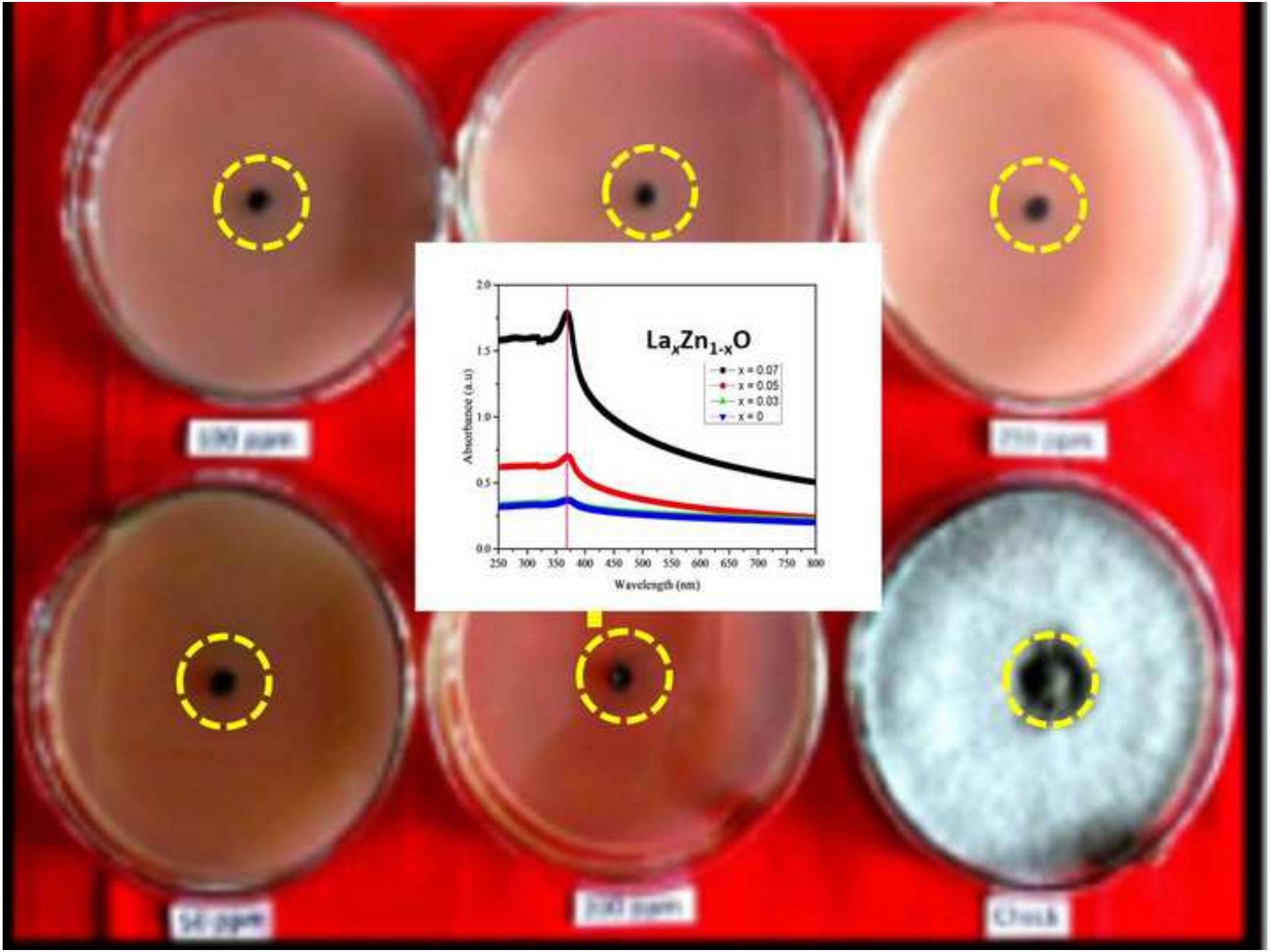

Highlights

- Enhanced optical properties La doped ZnO nanoparticles
- La-doped ZnO nanomaterials were synthesized by chemical method
- XRD, FT-IR, UV-Visible, HR-SEM, EDX, PL spectroscopy techniques were used
- The antibacterial activities of $La_xZn_{1-x}O$ were tested by modified disc diffusion method
- Average particle size of undoped and doped La-doped ZnO was found 15 to 10 nm